

Supporting Information

Bendable polymer electrolyte fuel cells using highly flexible Ag nanowire percolation network current collectors

Ikwhang Chang¹, Taehyun Park², Jinhwan Lee³, Min Hwan Lee⁴, Seung Hwan Ko^{3†}, and Suk Won Cha^{1,2†}

¹Graduate School of Convergence Science and Technology (GSCST), Seoul National University, Gwanakro 1 Gwanakgu, Seoul, 151744, Republic of Korea

²Dept. of Mechanical and Aerospace Engineering, Seoul National University, Gwanakro 1 Gwanakgu, Seoul, 151744, Republic of Korea

³School of Engineering, University of California, Merced, 5200 North Lake, Merced, California 95343, USA

⁴Department of Mechanical Engineering, Korea Advanced Institute of Science and Technology (KAIST), 291 Daehak-ro, Yuseong-gu, Daejeon, 305-701, Republic of Korea

Finite Element Analysis

When a flexible fuel cell (FFC) is subject to compression by the method indicated in Figure S1A, bending moment is generated because the lower part of the FFC is compressed and the upper part is stretched, as indicated in Figure S1B. In such a case, the FFC is bent upward, and this changes the direction of the compressive and tensile stresses which are initially laid horizontal to the curved direction, as described by the blue and red arrows in Figure S1B. The turned directions of the tensile and compressive stresses accordingly generate compressive clamping force vertical to the center layer where the membrane-electrode assembly (MEA) is located.

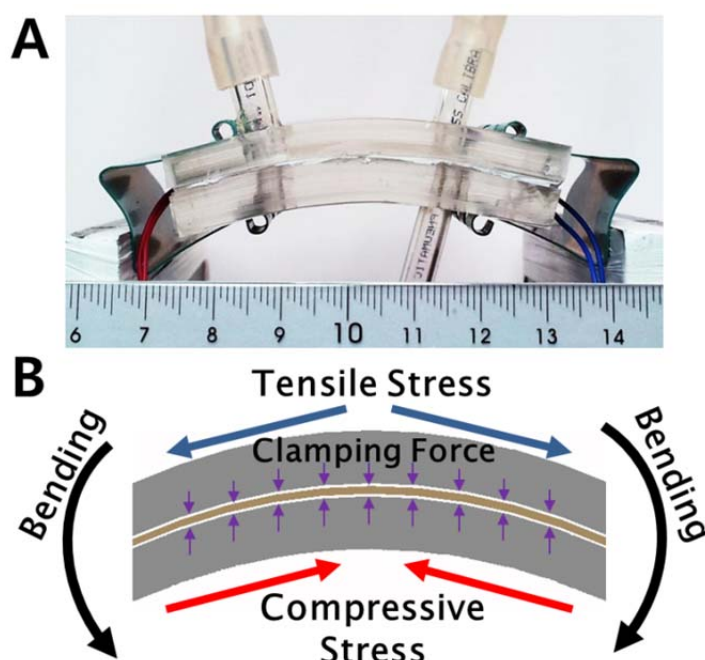


Figure S 1. A) Image of a bent flexible fuel cell. B) Schematic of the internal stress distribution in a flexible fuel cell by bending. Tensile stress in the upper side and compressive stress in the lower side generated by bending lead to compressive clamping force at the center part of the flexible fuel cell, where the membrane-electrode assembly is located.

In order to verify this concept, a finite element analysis (FEA) was applied to investigate the stress distribution inside the FFC. Comprehensive simulations were processed using COMSOL Multiphysics 4.2. Because the polydimethylsiloxane (PDMS) used in the experiment is an extremely elastic material, the Mooney-Rivlin (MR) model was applied, as it is used in many studies to calculate the solid mechanics of PDMS.^[1-3] The governing equations based on this model are as follows:

$$-\nabla \cdot \sigma = Fv, \sigma = (S \cdot (I + \nabla u))$$

$$S = \frac{\partial W_s}{\partial \varepsilon}$$

$$W_s = C_{10}(\bar{I}_1 - 3) + C_{01}(\bar{I}_2 - 3) + \frac{1}{2} \kappa (J_{el} - 1)^2$$

$$\varepsilon = \frac{1}{2} [(\nabla u)^T + \nabla u + (\nabla u)^T \nabla u]$$

Here, σ , W_s , κ , C_{10} , C_{01} , \bar{I}_1 , \bar{I}_2 , and u denote the Cauchy stress, the strain energy density, the bulk modulus, the first MR constant, the second MR constant, the first invariant of the unimodular component, the second invariant of the unimodular component, and the deformation, respectively. The material properties of the PDMS used in this study were as

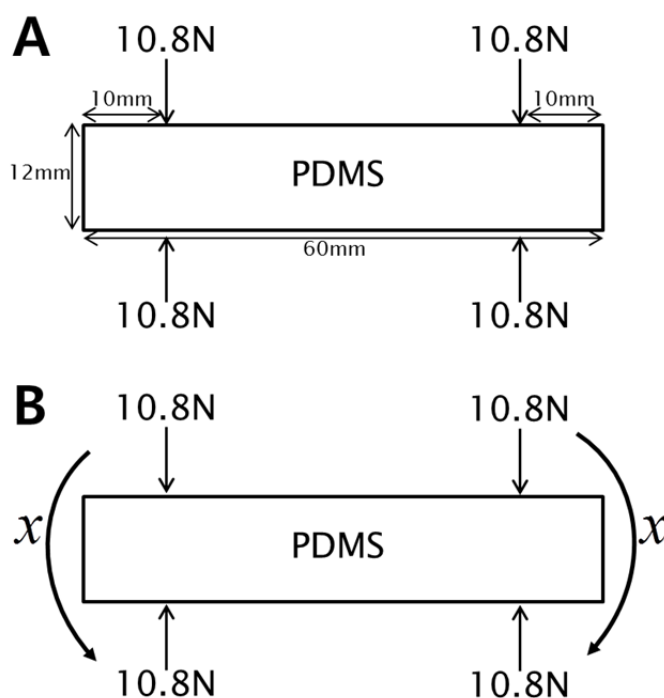


Figure S 2. A) Boundary conditions and dimensions of a flexible fuel cell with no bending. 10.8N was the forces exerted by the clamps. B) Bending of the flexible fuel cell was set as the parameter that controlled the total deformation of the cell. The bending was first applied to the positions where the clamping pressure was applied.

follows: density = 965 kg/m^3 , bulk modulus = 600 kPa, Poisson's ratio = 0.499, $C_{01} = 254$ kPa, and $C_{10} = 146$ kPa. [3-4] The Poisson's ratio was set to 0.499 rather than 0.5 to avoid divergence of the calculation.^[1]

The boundary conditions are indicated in Figure S2. The vertically compressing force, 10.8N, is the clamping forces by the clip, which were measured experimentally. As shown in Figure S1A, clamped spots were located 1 cm apart from the each edge. The dimensions of the width and height were 60 mm and 12 mm. In this case, although the total thickness of the FFC included the MEA, it was ignored because the thickness of the MEA is quite thin compared to 12 mm. The bending was therefore set as a parameter to control the deformation of the FFC.

Figure S3 shows the results of the stress analysis and actual images of the experiment. As expected, the internal stresses generated by bending propagated as the bending increased. In addition, Figure 5C shows the directions of the principal stresses; the internal compressive stresses vertical to the MEA were clearly visualized. The calculated forces are given in Figure 5D and, where it is evident that the ohmic/faradaic resistances and the average normal forces are negatively correlated.

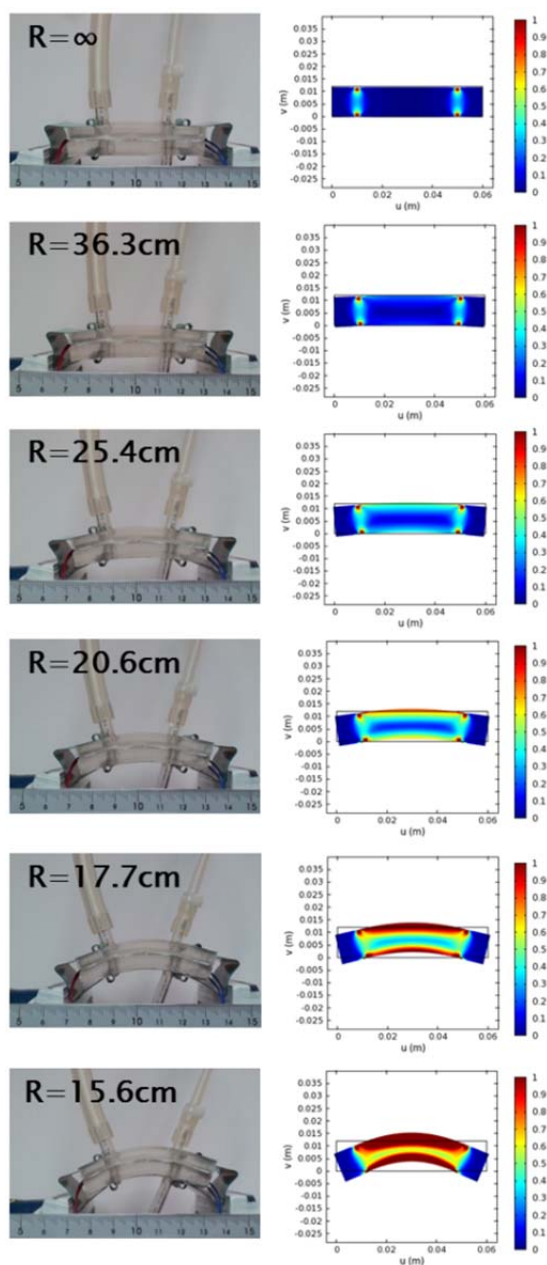


Figure S 3. Comparison of the experimental images and the simulation results. R denotes the bending radius of the fuel cell. $R = \infty$ is the initial position, where there is no bending of the fuel cell.

Durability test

As shown in Figure S4, this is a set of durability tests on the bendable fuel cell was also carried out. The power densities in Figure S4 A were the maximum power densities extracted from a full I-V sweep under every bending cycle. The impedance spectra were measured at a fixed dc bias of 0.5 V vs. OCV. More details on the bending conditions and measurement methods were presented as follows: bending cycles between 36.3 cm and 17.7 cm. Figure S4A shows the power density sharply decreases by 0.5 mW/cm² per cycle from 1 cycle to 25 cycles and by 0.1 mW/cm² per cycles after 25 cycles. The vertical arrows in Figure A show the cycles where impedance measurements were performed. The non-continuity of the measured power densities at these points are attributed to the disturbance caused by the impedance measurements. Figures S4B and S4C show impedance spectra measured under the bending radius of 36.3 cm and 17.7 cm, respectively. These spectra suggest that the ohmic loss increases with cycle continuously. However, the structure and morphologies of Ag NWs has not been changed significantly as shown in Figures S4D (as-prepared) and 1E (after 110 cycles). For further investigation of Ag NWs durability in Figure 1E, the electrical resistance of the long Ag NW cluster kept almost its initial value even after 2,000 cycles of bending; this result shows its initial and final resistances (see Figure S5). Further, even when the Ag NW/PDMS structure was mechanically extended by 157%, it maintained its good electrical conductivity. These results show that the electrical resistance of fabricated Ag NW percolation network electrode can be retained successfully under various harsh mechanical stresses including bending and stretching conditions. Given that, we confirmed that the delamination of MEA occur either between the GDL and catalyst layer or between the catalyst layer and membrane.

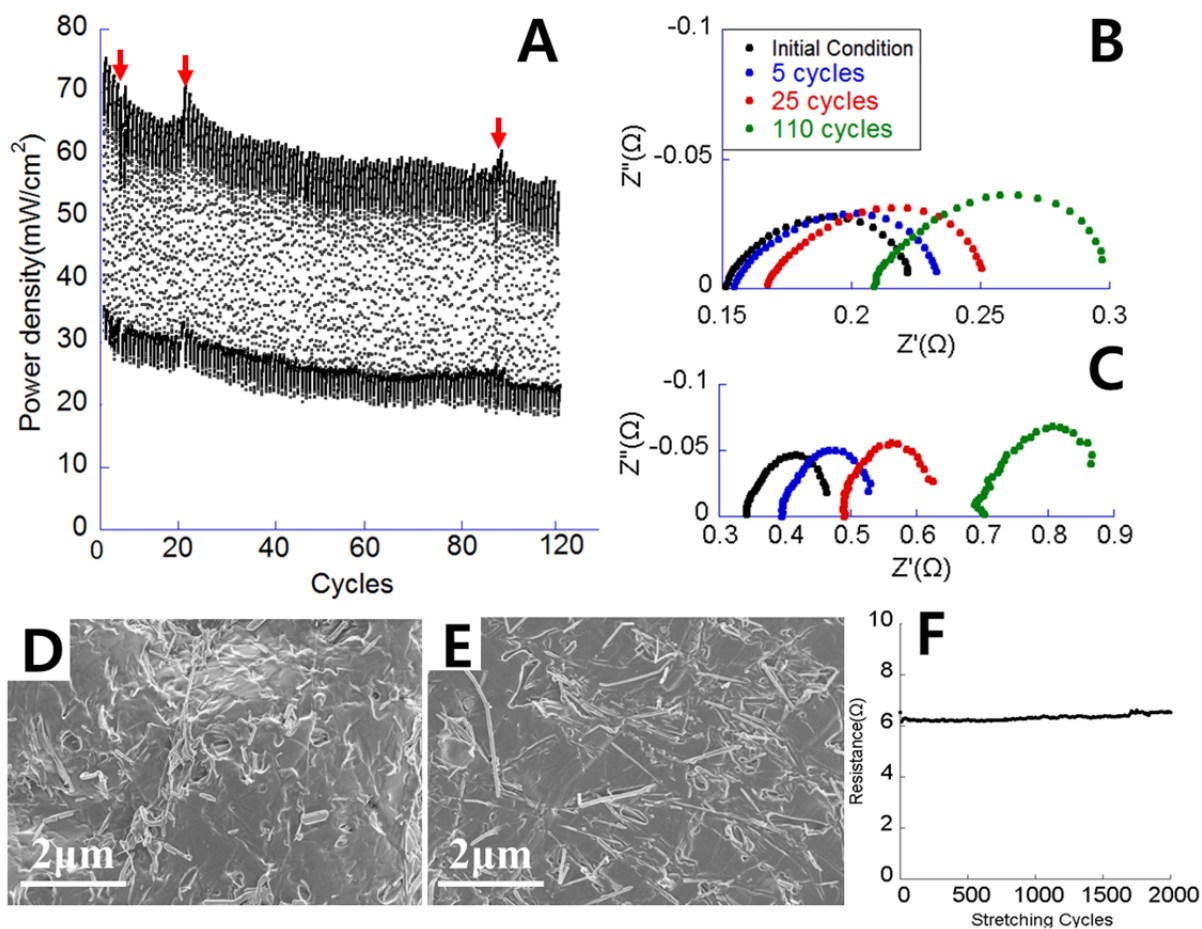


Figure S 4. A) Bending durability tests of 120 cycles. (Red arrows indicate, 5, 25, and 110 cycles). 5, 25, and 110 cycles impedance spectra of bendable fuel cell with $R=17.7$ cm bending radius (B), and $R=36.3$ cm bending radius (C). D) FESEM image of Ag NW percolation networks formed on PDMS at the initial condition. E) FESEM image of Ag NW on PDMS at the final condition. F) The measurement of Electrical resistance variation of Ag NW on PDMS during 2,000 cycles.

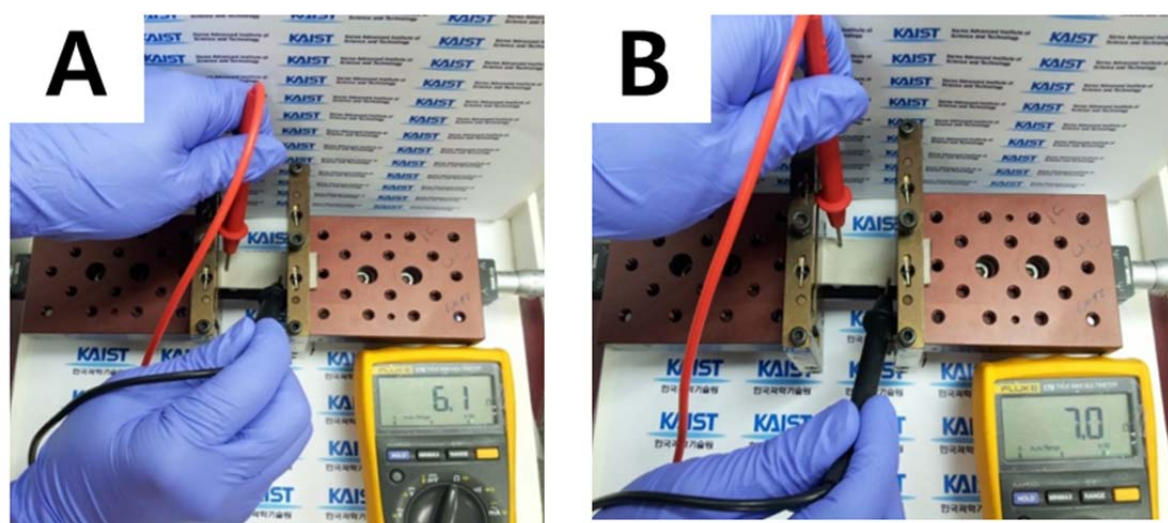


Figure S 5. Electrical resistance variation of Ag NW during 2000 cycles. Electrical resistance of the initial cycle (A) and the final cycle (B).

References

- [1] S. H. Yoon, V. Reyes-Ortiz, K. H. Kim, Y. H. Seo, M. R. K. Mofrad, *J. Microelectromech. S.* **2010**, *19*, 854.
- [2] Y. S. Yu, Y. P. Zhao, *J. Colloid Interf. Sci.* **2009**, *332*, 467.
- [3] S. Hosmane, A. Fournier, R. Wright, L. Rajbhandari, R. Siddique, I. H. Yang, K. T. Ramesh, A. Venkatesan, N. Thakor, *Lab Chip* **2011**, *11*, 3888.
- [4] S. J. Lee, J. C. Y. Chan, K. J. Maung, E. Rezler, N. Sundararajan, *J. Micromech. Microeng.* **2007**, *17*, 843.